Title
Crystal structure of phospholipase A2 from Indian cobra reveals a trimeric association.

Journal
Proceedings of the National Academy of Sciences of the United States of America, 90(1)

ISSN
0027-8424

Authors
Fremont, DH
Anderson, DH
Wilson, IA
et al.

Publication Date
1993

DOI
10.1073/pnas.90.1.342

Peer reviewed

Proc. Natl. Acad. Sci. USA
Vol. 90, pp. 342–346, January 1993
Biochemistry

Crystal structure of phospholipase A_2 from Indian cobra reveals a trimeric association

(x-ray crystallography/protein structure/protein trimer/molecular replacement)

DAVED H. FREMONT*†, DANIEL H. ANDERSON*, IAN A. WILSON†, EDWARD A. DENNIS*‡, AND NGUYEN-HUU XUONG*

*Department of Chemistry, University of California, San Diego, La Jolla, CA 92093; and †Department of Molecular Biology, The Scripps Research Institute, 10666 North Torrey Pines Road, La Jolla, CA 92037

Communicated by Joseph Kraut, July 13, 1992

ABSTRACT **Phospholipase A_2 (PLA_2) from Indian cobra venom (*Naja naja naja*) was crystallized from ethanol in space group $P4_32_12$ in the presence of Ca^{2+}. The x-ray crystal structure was determined to 2.3-Å resolution by molecular replacement techniques using a theoretical model constructed from homologous segments of the bovine pancreatic, porcine pancreatic, and rattlesnake venom crystal structures. The structure was refined to an R value of 0.174 for 17,542 reflections between 6.0- and 2.3-Å resolution ($F > 2\sigma$), including 148 water molecules. The 119-amino acid enzyme has an overall architecture strikingly similar to the other known PLA_2 structures with regions implicated in catalysis showing the greatest structural conservation. Unexpectedly, three monomers were found to occupy the asymmetric unit and are oriented with their catalytic sites facing the pseudo-threefold axis with ≈15% of the solvent accessible surface of each monomer buried in trimer contacts. The majority of the interactions at the subunit interfaces are made by residues unique to PLA_2 sequences from cobra and krait venoms. The possible relevance of this unique trimeric structure is considered.**

Phospholipase A_2 (PLA_2) catalyzes the cleavage of the 2-acyl ester bond of phospholipids in a Ca^{2+}-dependent reaction (1). PLA_2 is found both extracellularly, serving digestive and other functions, and intracellularly, where it is implicated in the regulation of prostaglandins and leukotrienes through the release of arachidonic acid (2). PLA_2 has also been found in various snake venoms, where it is thought to work synergistically with nonenzymatic toxins (3). PLA_2 sequences fall into two major groups based upon the location of their cysteine residues (4). Indian cobra PLA_2, composed of 119 amino acids and containing 7 disulfide bonds, belongs to group IA, which is distinguished from group IB (from mammalian pancreatic tissues) because of a shorter surface-exposed loop. PLA_2 sequences from vipers and rattlesnakes and those secreted from mammalian nonpancreatic tissues belong to group II. It has been estimated that the ancestral genes for these two distinct groups diverged more than 200 million years ago (3).

The crystal structures of PLA_2 have been determined from a number of sources, including bovine pancreas (5), porcine pancreas (6), rattlesnake venom (7), Chinese cobra venom (8), bee venom (9), eastern cottonmouth venom (10), and human synovial fluid (11, 12). All of these structures share key features implicated in phospholipid hydrolysis. Most notable is the conservation of His-48 and Asp-99, which in conjunction with a bound water had been predicted to operate with a catalytic mechanism similar to that found in the serine proteases (13). This hypothesis is supported by four recently solved PLA_2–inhibitor complexes, one with a substrate-derived amide analogue (14) and three with a transition-state analogue (9, 10, 12).

The oligomeric state of PLA_2 during catalysis is open to question (15). The PLA_2 from rattlesnake venom has been shown by both biochemical and crystallographic evidence to associate as a dimer (16), while the mammalian pancreatic enzymes are monomeric (6). Several studies suggest that phospholipid induces aggregation of the otherwise monomeric cobra venom PLA_2 (17–19).

In the current study, we have determined the high-resolution three-dimensional structure of Indian cobra PLA_2 to further our understanding of the biochemistry underlying its function. In the course of this study innovative molecular replacement methodologies were developed and used. Analysis of this PLA_2 structure reveals that the enzyme associates as a trimer under the crystallization conditions used, which may be indicative of an unusual regulatory mechanism.

MATERIALS AND METHODS

Enzyme Preparation and Crystallization. PLA_2 was purified from *Naja naja naja* cobra venom (Pakistan) obtained from the Miami Serpentarium (20). Initial seed crystals were grown by microdialysis of 10 mg of PLA_2 per ml against 20% (vol/vol) ethanol/5 mM $CaCl_2$/50 mM Tris·HCl, pH 8. The PLA_2 seed crystals were stored at 4°C in an artificial mother liquor containing 20% ethanol, 15% (wt/vol) polyethylene glycol 6000 (Baker), 5 mM $CaCl_2$, and 25 mM Tris·HCl (pH 8) (21). The crystals used for data collection were grown at 16°C by a repeat seeding microdialysis protocol (22). The crystals obtained are of tetragonal space group $P4_32_12$, with unit cell dimensions $a = b = 88.6$ Å and $c = 107.4$ Å. The solvent content of the crystal was calculated (23) as 56% ($V_m = 2.8$) with three molecules in the asymmetric unit.

Data Collection. X-ray diffraction data were collected on a single crystal using the University of California, San Diego, Mark II multiwire detector (24). A total of 226,069 observations were measured and subsequently reduced to 19,602 unique reflections (25). Only 69 of the theoretically possible reflections were not recorded to 2.3 Å, and 91.6% of the observations had an I/σ value of >2.0. These data merged to an R_{sym} of 4.7% on intensities.

Structure Prediction. A theoretical model of Indian cobra PLA_2, CM22, was constructed from the predicted homologous segments of porcine [Protein Data Base entry 1P2P (6)] and rattlesnake [(1PP2) (7)] crystal structures grafted onto the primary framework of the bovine [1BP2 (5)] structure. Spe-

The publication costs of this article were defrayed in part by page charge payment. This article must therefore be hereby marked "*advertisement*" in accordance with 18 U.S.C. §1734 solely to indicate this fact.

Abbreviation: PLA_2, phospholipase A_2.

‡To whom reprint requests should be addressed at: Department of Chemistry, 0601, University of California, San Diego, 9500 Gilman Drive, La Jolla, CA 92093-0601.

cifically, rattlesnake residues Ile-12 through Gly-18 (residue numbering from ref. 26) and porcine residues His-117 through Cys-126 were thought to better model the Indian cobra sequence and served to replace the equivalent residues of the bovine structure. The crude model was completed by deleting loop residues Lys-62 through Asp-66 and adding the C-terminal glutamine. The Ca^{2+} of 1BP2 was maintained. Initial side-chain torsion angles for the model were transferred directly from the parent models when an analogous residue was present; otherwise, the preferred rotamers were taken from the BIOSYM residue library. This model was then solvated and subjected to several rounds of both steepest descents and conjugate gradient energy minimization by using the program DISCOVER (Biosym, San Diego) running on a Convex C210 supercomputer. Regions of the model with poor geometry or steric clashes were periodically rebuilt.

Molecular Replacement. Crowther (27) self and cross-rotation function analysis was performed by using the program MERLOT (28) with data between 10.0- and 3.0-Å resolution and a Patterson cutoff radius of 17 Å. Cross-rotation functions were carried out with four models (1BP2, 1PP2, 1P2P, and CM22).

Translation-function calculations were performed by using a fast Fourier transform-based full cell search with code developed by David Filman and Jairo Arevalo based on an algorithm derived by Harada *et al.* (29) and using code previously developed by Steigemann (30). A typical calculation was carried out on a 0.5-Å grid by employing structure factors calculated in a P1 cell using data between 8.0 and 4.0 Å.

Atomic Refinement. Rigid-body, least-squares, and simulated-annealing refinements of Indian cobra PLA_2 were carried out with the program XPLOR (31) executed on both Convex and Cray supercomputers. An atomic model was fitted to both $2F_o - F_c$ electron-density maps and $F_o - F_c$ omit maps displayed on a Personal Iris workstation running the molecular modeling program FRODO (32). Omit maps were typically calculated by removing 30-residue segments of the model (≈10% of the asymmetric unit) followed by least-squares atomic refinement and map calculation.§

RESULTS AND DISCUSSION

Structure Determination. The structure determination of Indian cobra PLA_2 was initially undertaken by the technique of multiple isomorphous replacement. Data were collected on crystals containing both uranyl and mercury derivatives (21). However, before the structure was solved by heavy-atom methods, the coordinates of PLA_2 from other species became available. Of the available structures, the sequence similarity of bovine pancreatic PLA_2 is highest (58%), closely followed by porcine (56%), while the rattlesnake is more distantly related (39%). As a first step in the process, the chimeric model CM22 was built. The construction of such a model served two purposes: (*i*) to aid in the molecular replacement rotation and translation function analysis and (*ii*) to facilitate the atomic model building and refinement.

The most surprising result of the structural analysis was the finding of three PLA_2 molecules in the asymmetric unit related by approximate threefold symmetry. Both the solvent content and the self-rotation function (Fig. 1) are consistent with three molecules in the asymmetric unit. The Matthews coefficient for the trimer, $V_m = 2.7$, is well within the range observed for other crystallized globular proteins, whereas the value calculated for the dimer, $V_m = 4.1$, falls outside the range typically observed (23). Noncrystallographic symmetry peaks can be seen in the twofold, threefold, and fourfold sections of the self-rotation function, each appearing at ≈60% of the height of the crystallographic peaks (Fig. 1). The best explanation is that the crystal contains a noncrystallographic threefold symmetry that, when combined with tetragonal crystallographic operators, produces the observed twofold and fourfold symmetry peaks seen in the self-rotation function maps. Indeed, the matrix corresponding to a crystallographic twofold operator ($\phi = 90°$, $\psi = 90°$, $\kappa = 180°$), when operating on the approximate noncrystallographic operator ($\phi = 180°$, $\psi = 55°$, $\kappa = 120°$), produces one of the observed twofold noncrystallographic symmetry peaks ($\phi = 45°$, $\psi = 45°$, $\kappa = 180°$).

Cross-rotation function analysis resulted in three peaks related by the observed noncrystallographic symmetry. Peaks corresponding to monomer A and B were consistently seen as the strongest in the Crowther map for all four models, whereas the peak corresponding to monomer C was considerably weaker, regardless of resolution range or starting probe model orientation employed. The use of multiple models in the cross-rotation function, which is routinely carried out in our laboratory for Fab structure determinations (33), proved effective in confirming the correctness of these solutions. The CM22 model appeared to be the best model based upon the absolute values of the peak heights in these rotation studies.

Attempts were made to position all three oriented CM22 models in the two enantiomeric space groups. In only one case was a possible solution found that was 1.0 σ above the next highest peak in the translation search (that for the monomer A in $P4_32_12$). To position a second molecule, an electron-density overlap algorithm similar to that described (34) was used. A $2F_o - F_c$ map was calculated with only the correctly positioned monomer as the phasing model, with the F_c density for that model subsequently subtracted from the map. An F_c map was then calculated for the model in orientation B, and a real space statistical search, based upon electron-density overlap, was performed. The resultant peak list contained a completely unambiguous solution. The third monomer was positioned into the unit cell visually on an Iris workstation based upon the threefold symmetry and was confirmed by an $F_o - F_c$ map calculated in the absence of its coordinates. The R value of the crudely positioned monomers at this stage was 0.49 for data between 12- and 4-Å resolution. These results clearly show the power of the molecular replacement technique, where only a third of the scattering matter of the asymmetric unit was necessary to properly position the probe model.

Model building of the trimer into both $2F_o - F_c$ and $F_o - F_c$ omit maps proceeded smoothly, with the primary exception of the C-terminal residue Gln-127, the Ca^{2+}-binding loop residues Gly-30 and Arg-31, and turn residues Ser-78, Gln-79, and Gly-80, all of which exhibited poorly ordered density. Gros *et al.* (35) found these same regions exhibited significantly larger atomic fluctuations in bovine pancreatic PLA_2. During the initial stages of atomic refinement only monomer A was independently built, while monomers B and C were forced to adopt the same conformation as monomer A by using noncrystallographic weighting of the atomic positions. The trimer refinement scheme used was similar to that employed by Weis *et al.* (36). The final cycles of refinement and rebuilding used no symmetry weighting schemes.

Individual temperature factors were calculated after the R value had reached a value of 0.28. The electron density for monomer B was in general more difficult to interpret than for either monomer A or C, and, not surprisingly, its temperature factors were considerably higher. The average temperature factor at the end of refinement for monomer B was ≈40 $Å^2$, while both monomer A and C had values of 25 $Å^2$. Very little electron density was observed for either the C-terminal Gln-127 or the side chain of Arg-31 for any of the monomers.

§The atomic coordinates have been deposited with the Protein Data Bank, Chemistry Department, Brookhaven National Laboratory, Upton, NY 11973 and will be available for prerelease.

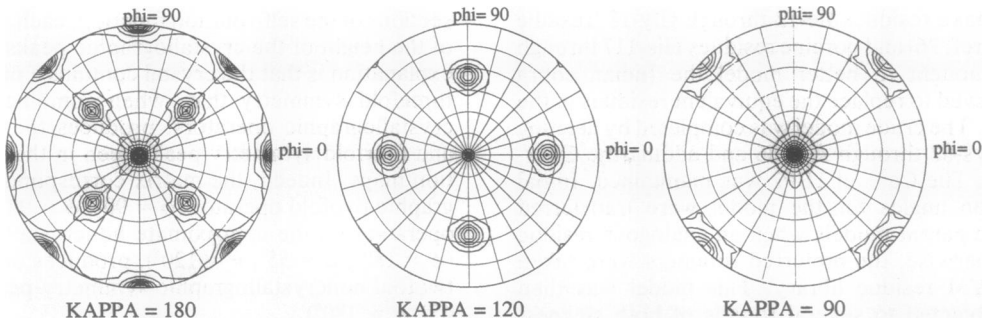

FIG. 1. Polar-angle self-rotation contour plots showing the twofold, threefold, and fourfold symmetry operators (κ = 180°, 120°, and 90°, respectively). Contour lines are drawn at 10% intervals of the origin peak. Noncrystallographic symmetry peaks can be seen in all three sections at roughly 60% of the true crystallographic peaks. Contour plots were prepared by code developed by Todd Yeates (University of California, Los Angeles).

The density for the Ca^{2+} atom was unambiguous in all three monomers, but the backbone of the binding loop had a few main-chain discontinuities, especially in monomer B. The density for residues 78–80 became more interpretable in later stages of rebuilding. Solvent molecules were added late in refinement after the R value had reached 0.20. The current R value is 0.174 for 17,542 reflections between 6.0- to 2.3-Å ($F > 2\sigma$), including 148 water molecules. The rms deviation from ideal bond lengths is 0.013 Å and from ideal angles is 2.94°. The final electron density maps are of good quality (Fig. 2).

Description of the Structure. The overall fold of the Indian cobra PLA_2 is strikingly similar to the pancreatic enzymes and that of the rattlesnake. The 119-amino acid protein consists of three major (residues 2–12, 40–55, and 90–107) and two minor (19–23 and 122–125) α-helical segments, a double-stranded antiparallel β-sheet known as the β-wing (75–84), a Ca^{2+}-binding loop (25–35), and seven disulfide bonds (11:77, 27:126, 29:45, 44:105, 51:98, 61:91, 84:96). The two longest helices, 40–55 and 90–107, are antiparallel (Fig. 3). Ca^{2+} is coordinated to seven ligands, which form an oxygen cage. The carbonyl oxygens of Tyr-28, Gly-30, and Gly-32, the carboxylate oxygens of Asp-49, and two water molecules bind in positions nearly identical to those found in the pancreatic structures.

In the porcine mutant PLA_2–inhibitor complex (14), extensive hydrophobic interactions between the substrate analogue and PLA_2 were observed (residues Leu-2, Phe-5, Ile-9, Leu-19, Phe-22, Tyr-52, Cys-29, and Cys-45). Of these eight residues, only Leu-19 is different in the Indian cobra sequence. A comparison of Indian cobra PLA_2 with the porcine pancreatic mutant structure (3P2P) shows these conserved hydrophobic residues are virtually superimposable upon each other. A wall of hydrophobic residues forms the core of the enzyme. (Fig. 4.) Those residues implicated in the catalytic network (His-48, Tyr-52, Tyr-69, and Asp-99) are likewise completely conserved, although the orientation of the side chain of Tyr-69 is slightly different, both between the porcine and Indian cobra enzyme and among the various monomers. In Chinese cobra PLA_2 (8), Tyr-69 binds to the *sn*-3 phosphate of the transition-state analogue, and it was proposed that its role in catalysis was that of a mobile hydrophobic "flap." This same interaction was observed in the porcine mutant PLA_2–inhibitor complex (14). The different orientations of Tyr-69 found in the three Indian cobra PLA_2 monomers, most notable for monomer B in which it differs by 30° from monomer A, seems to support the proposition that the flap is secured firmly only when the substrate is productively bound (38).

Scott *et al.* (38) have proposed that a second Ca^{2+} serves as a supplemental electrophile in the enzymatic mechanism. In the unliganded Chinese cobra PLA_2, Ca^{2+} is found loosely interacting with the side chains of Asp-24 and Asn-119. There is no evidence for a second Ca^{2+} site in the trimeric Indian cobra structure. However, Asp-24 has been found to be in an intermolecular salt bridge with Arg-31 at the interface of the trimer, although the density for Arg-31 is weak. The crystallization conditions of the Chinese cobra enzyme contained 10 mM Ca^{2+}, whereas the crystals employed herein were grown at half that concentration and were sensitive to any further increase. It may well be that the displacement of the salt bridge by a bound Ca^{2+} at Asp-24 would destabilize the trimer.

Trimeric Association. The three Indian cobra PLA_2 molecules in the asymmetric unit are related by a pseudo-threefold axis (Fig. 4). The rotation necessary to superimpose monomer A onto monomer B is 124°, while the rotation from monomer A to monomer C is 117°. The monomers pack with the antiparallel set of helices on the outside ≈45° tilted from being coincident with the threefold axis. The trimer contacts involve primarily electrostatic interactions. The residues whose side chains are involved in these intersubunit contacts (Tyr-3, Lys-6, Asp-24, Arg-31, Glu-56, Asn-119, Asp-121, and Lys-123) are unique to sequences for enzymes from the Elapidae family (i.e., group IA sequences from African and Asian cobras and kraits) (3). A hydrogen bond is clearly seen at all three interfaces between the hydroxyl group of Tyr-3 and the amide nitrogen of Tyr-69. There are two primary hydrophobic contacts seen in the trimer interfaces, both

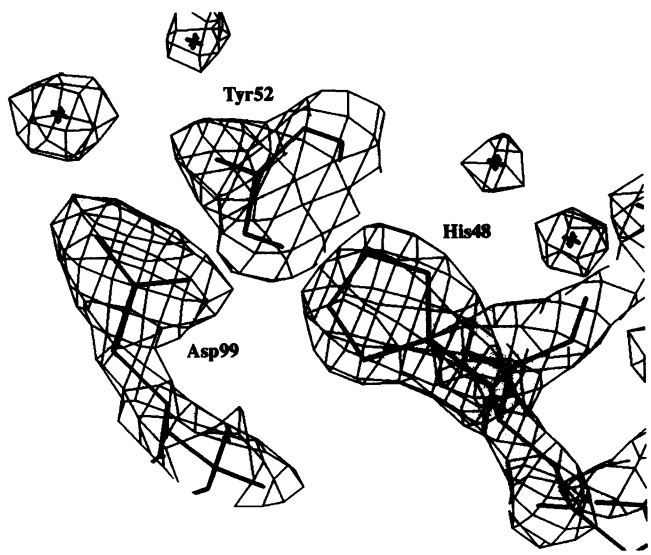

FIG. 2. $2F_o - F_c$ electron-density map contoured at 2σ corresponding to the region surrounding the catalytic His-48. Four well-ordered water molecules can be seen in this view of the catalytic site.

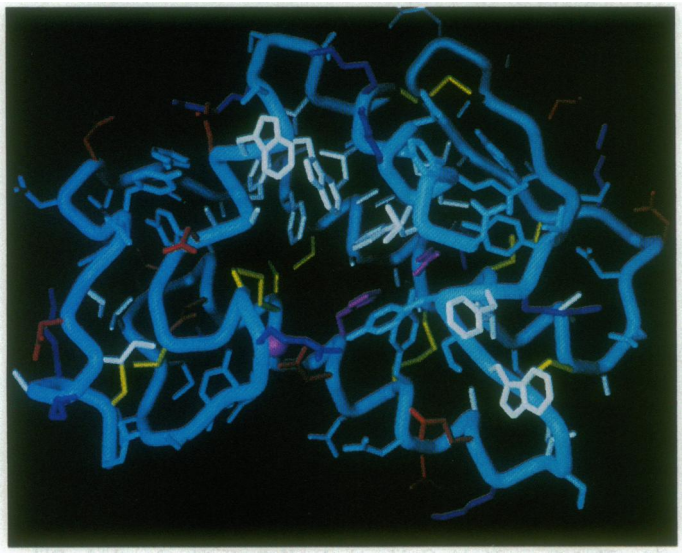

FIG. 3. Structure of the refined Indian cobra PLA_2 (monomer A). Color scheme of the tube (37) figure: protein backbone and uncharged hydrophilic residues in cyan; hydrophobic residues in white; disulfide bonds in yellow; arginine and lysine in blue; glutamic acid and aspartic acid in red; and His-48, Asp-99, and Ca^{2+} in magenta.

involving residues unique to the Elapidae family. Trp-20 packs tightly against the backside of the Ca^{2+}-binding loop at Gly-30, while Trp-67 makes extensive contacts with the phenolic ring of Tyr-3. It seems extremely unlikely that the PLA_2 from any other species besides cobra or krait could form similar trimeric contacts.

The center of the trimer is composed of a large solvent pore ≈30 Å long and between 10 Å and 4 Å wide (Fig. 4). The lip of one side of the pore is made from symmetrically related Arg-31–Asp-24 salt bridges, while at the other side Phe-70 from all three monomers packs into the center to form a sort of nozzle. One of the most conspicuous features of the pore is the lack of any electron density corresponding to either bound solvent or ions. Of the 148 identified water molecules, none are found to be associated with the internal cavity. In contrast, many waters have been identified on the outer surface of the trimer. The three catalytic networks are symmetrically situated near the center of the pore facing towards the threefold axis. None of the residues implicated in catalysis are in direct trimer contacts. Although the active site appears unobstructed by neighboring monomers, it may well be that substrate is incapable of reaching the interior of the pore.

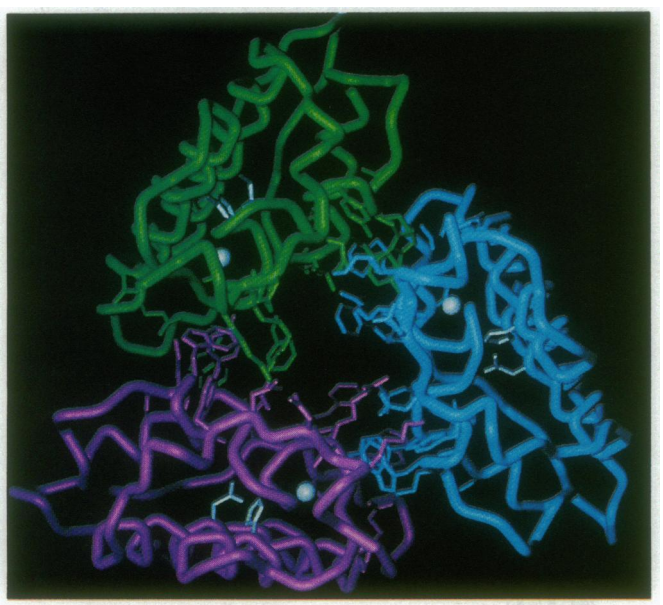

FIG. 4. Trimeric packing of the three monomers of Indian cobra PLA_2 in the asymmetric unit. The backbone is represented by a continuous tube (37). Side chains are shown for residues that make interfacial van der Waals contact. His-48, Asp-99, and Ca^{2+} are shown in white for each of the monomers.

Each Indian cobra monomer was calculated (ref. 39, with a 1.4-Å probe) to have ≈6900 $Å^2$ of solvent-accessible area. A full 15% of this area is found to be buried in the interface of the trimer. This compares favorably with the surface areas buried in known multimeric proteins (40). A similar calculation of the rattlesnake crystal structure shows 18% of each monomer's surface is buried in dimer contacts. In contrast, the porcine mutant structure has two molecules in the asymmetric unit and only 6% of the monomer surface is buried in noncrystallographic contacts.

Structural Alignment. A major difference in the Cobra structure from those previously described occurs in the connecting region between the N-terminal helix and the Ca^{2+}-binding loop, specifically in the region of Trp-19 and Trp-20. The initial hypothesis of the modeling study was that an amino acid deletion in this region relative to the pancreatic structures would occur at the same location (position 15) as found in the rattlesnake structure. However, structural alignment (26, 41) indicates instead a deletion at position 18 in the Indian cobra structure. The concomitant residue deletion and substitution of two bulky tryptophan residues, which are specific to PLA_2 sequences from the Elapidae family, results in a local rearrangement of the polypeptide backbone, which may well affect the oligomerization state of the enzyme, since Trp-20 is involved in intersubunit contacts. In their attempts to model the structure of a cobra venom PLA_2, Demaret *et al.* (42) also wrongly assumed that the cobra deletion would occur at position 15.

Elapid Versus Pancreatic Loop. The largest difference between the various PLA_2 structures occurs in the surface loop connecting the second major helix with the β-wing. In an unusual mutagenesis experiment, Kuipers *et al.* (43) engineered a porcine PLA_2 containing the loop observed in several cobra structures by deleting residues 62–66 and changing Asp-59 → Ser, Ser-60 → Gly, and Asn-67 → Tyr. The Indian cobra sequence differs from this newly created loop only at Trp-67. There is no consensus residue for position 67 in group I snakes containing the "elapid" loop, although both tyrosine and tryptophan occur quite frequently (3). The engineered PLA_2 was shown to exhibit up to a 16-fold increase in hydrolysis of aggregated short-chain lecithins relative to the wild-type porcine enzyme (43). In a remarkable confirmation of this experiment, the loops seen in the porcine mutant and the Indian cobra structure reported here are virtually identical (Fig. 5).

Implications of Trimeric Structures. Cobra venom PLA_2 has been shown to undergo a concentration-dependent aggregation to dimeric or higher order aggregates (18). While the enzyme appears monomeric in dilute solution at concentrations expected to occur physiologically or where kinetic assays are carried out ($<<1$ μM), evidence suggests that phospholipid substrates induce aggregation of the otherwise monomeric enzyme (18, 19). Unfortunately, none of these approaches can distinguish whether the functional subunit is a monomer or higher order aggregate. The finding of a trimeric association raises several interesting possibilities. It could itself represent the active aggregated form of the enzyme or at least indicate the potential contact points and structural features of an aggregated catalytically active form of the enzyme.

In contrast, the trimeric form could represent an inactive form of the enzyme. While this oligomeric state may well

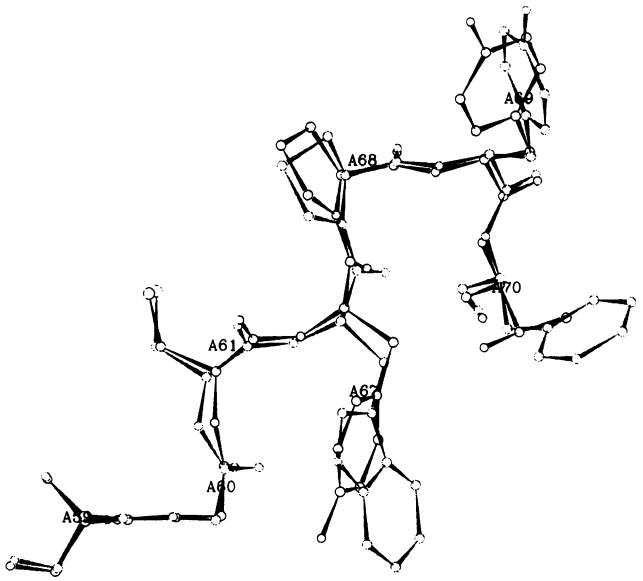

FIG. 5. Structure of the elapid loop of Indian cobra PLA_2 (lightly shaded) and an engineered porcine pancreatic PLA_2 (darkly shaded). The Indian cobra loop contains tryptophan at position 67. The backbone atoms of Indian cobra monomer A residues Ser-59 through Phe-70 were superimposed onto the analogous residues of the engineered structure [3P2P (43)] with a rms deviation of 0.32 Å.

have no functional significance in the catalytic process *per se*, it could well occur *in vivo* as a mechanism to maintain the protein in an inactive state in the cobra or krait snake venom sacks, where it occurs at high concentrations. Although the other group I structures from mammalian sources (group IB) are known to be produced as proenzymes requiring cleavage of the N terminus for activation, group IA PLA_2 structures from snakes do not. Perhaps this novel oligomeric state, if it indeed does occur *in vivo*, has evolved to produce the same functional effect as the proenzyme leader sequence, namely, to keep the enzyme dormant until its activity is required.

In conclusion, the observed crystal structure of Indian cobra PLA_2 exhibits an unusual and unexpected oligomeric state that could be physiologically relevant in either promoting or inhibiting its activities. Crystals of Indian cobra PLA_2 have recently been characterized in a different spacegroup, grown with different solvent conditions (B. W. Segelke, I.A.W., E.A.D., and Ng.-H.X., unpublished data). Interestingly, PLA_2 forms the same trimer in these crystals as a result of true crystallographic symmetry, lending credence to the notion that the trimeric structure may be a functionally important feature of Indian cobra PLA_2.

We thank Todd Yeates, Robyn Stanfield, and Suzanne Rutherford for stimulating discussions and insights; David Filman and Jairo Arevalo for their phased-translation function; Chris Nielson, Victor Ashford, Ron Hamlin, and Don Sullivan for aid in data collection and processing; and Florence Davidson and Raymond Deems for protein preparations. This work was supported in part by National Institutes of Health Grants CA-09523 (to D.H.F.), RR01644 (to Ng.-H.X.), GM-38794 (to I.A.W.), and GM-20501 (to E.A.D.); National Science Foundation Grant DMB-88-17392 (to E.A.D.), and the Markey Charitable Trust (to Ng.-H.X.).

1. Dennis, E. A. (1983) in *The Enzymes*, ed. Boyer, P. (Academic, New York), Vol. 16, pp. 423–446.
2. Dennis, E. A. (1987) *Bio/Technology* **5**, 1294–1300.
3. Davidson, F. F. & Dennis, E. A. (1990) *J. Mol. Evol.* **31**, 228–238.
4. Heinrikson, R. L., Krueger, E. T. & Keim, P. S. (1977) *J. Biol. Chem.* **252**, 4913–4921.
5. Dijkstra, B. W., Kalk, K. H., Hol, W. G. J. & Drenth, J. (1981) *J. Mol. Biol.* **147**, 93–123.
6. Dijkstra, B. W., Renetseder, R., Kalk, K. H., Hol, W. G. J. & Drenth, J. (1983) *J. Mol. Biol.* **168**, 163–179.
7. Brunie, S., Bolin, J., Gewirth, D. & Sigler, P. B. (1985) *J. Biol. Chem.* **260** (17), 9742–9749.
8. White, S. P., Scott, D. L., Otwinowski, Z., Gelb, M. & Sigler, P. B. (1990) *Science* **250**, 1560–1563.
9. Scott, D. L., Otwinowski, Z., Gelb, M. & Sigler, P. B. (1990) *Science* **250**, 1563–1566.
10. Holland, D. R., Clancy, L. L., Muchmore, S. W., Ryde, T. J., Einspar, H. M., Finzel, B. C., Heinrikson, R. L. & Watenpaugh, K. D. (1990) *J. Biol. Chem.* **265** (29), 17649–17656.
11. Wery, J. P., Schevitz, R. W., Clawson, D. K., Bobbitt, J. L., Dow, E. R., Gamboa, G., Goodson, T., Herman, R. B., Kramer, R. M., McClure, D. B., Mihelich, E. D., Putman, J. E., Sharp, J. D., Stark, D. H., Teater, C., Warrick, M. W. & Jones, N. D. (1991) *Nature (London)* **352**, 79–82.
12. Scott, D. L., White, S. P., Browning, J. L., Rosa, J. J., Gelb, M. H. & Sigler, P. B. (1991) *Science* **254**, 1007–1010.
13. Dijkstra, B. W., Drenth, J. & Kalk, K. H. (1981) *Nature (London)* **289**, 604–606.
14. Thunnissen, M. M. G. M., Ab, E., Kalk, K. H., Drenth, J., Dijkstra, B. W., Kuipers, O. P., Dijkman, R., de Haas, G. H. & Verheij, H. M. (1990) *Nature (London)* **347**, 689–691.
15. Roberts, M. F., Deems, R. A. & Dennis, E. A. (1977) *Proc. Natl. Acad. Sci. USA* **74**, 1950–1954.
16. Keith, C., Feldman, D. S., Deganello, S., Glick, J., Ward, K. B., Jones, G. D. & Sigler, P. B. (1981) *J. Biol. Chem.* **256**, 8602–8607.
17. Pluckthun, A. & Dennis, E. A. (1985) *J. Biol. Chem.* **260**, 11099–11106.
18. Hazlett, T. L. & Dennis, E. A. (1985) *Biochemistry* **24**, 6152–6158.
19. Lombardo, D. & Dennis, E. A. (1985) *J. Biol. Chem.* **260**, 16114–16121.
20. Hazlett, T. L. & Dennis, E. A. (1985) *Toxicon* **23**, 457–466.
21. Anderson, D. H. (1986) Ph.D. dissertation (University of California, San Diego).
22. Thaller, C., Eichele, G., Weaver, L. H., Wilson, E., Karlsson, R. & Jansonius, J. N. (1985) *Methods Enzymol.* **114**, 132–135.
23. Matthews, B. W. (1968) *J. Mol. Biol.* **33**, 491–497.
24. Hamlin, R. (1985) *Methods Enzymol.* **114**, 416–452.
25. Howard, A. J., Nielson, C. & Xuong, N.-H. (1985) *Methods Enzymol.* **114**, 452–472.
26. Renetseder, R., Brunie, S., Dijkstra, B. W., Drenth, J. & Sigler, P. B. (1985) *J. Biol. Chem.* **260** (21), 11627–11634.
27. Crowther, R. A. (1972) in *The Molecular Replacement Method*, ed. Rossmann, M. G. (Gordon & Breach, New York), pp. 173–178.
28. Fitzgerald, P. D. M. (1988) *J. Appl. Crystallogr.* **21**, 273–278.
29. Harada, Y., Lifchitz, A. & Berthou, J. (1981) *Acta Crystallogr. Sect. A* **37**, 398–406.
30. Steigemann, W. (1982) *PROTEIN Package* (Max-Planck-Institute for Biochemistry, Martinsried, F.R.G.).
31. Brunger, A. T., Kuriyan, J. & Karplus, M. (1987) *Science* **235**, 458–460.
32. Jones, T. A. (1978) *J. Appl. Crystallogr.* **11**, 268–272.
33. Wilson, I. A., Rini, J. M., Fremont, D. H., Fieser, G. G. & Stura, E. A. (1991) *Methods Enzymol.* **203**, 153–176.
34. Read, R. J. & Schierbeek, A. J. (1988) *J. Appl. Crystallogr.* **21**, 490–495.
35. Gros, P., van Gunsteren, W. F. & Hol, W. G. J. (1990) *Science* **249**, 1149–1152.
36. Weis, W. I., Brunger, A. T., Skehel, J. J. & Wiley, D. C. (1990) *J. Mol. Biol.* **212**, 737–761.
37. Connolly, M. L. (1985) *J. Mol. Graphics* **3**, 19–24.
38. Scott, D. L., White, S. P., Otwinowski, Z., Yuan, W., Gelb, M. & Sigler, P. B. (1990) *Science* **250**, 1541–1546.
39. Kabsch, W. & Sander, C. (1983) *Biopolymers* **22**, 2577–2637.
40. Miller, S., Lesk, A. M., Janin, J. & Chothia, C. (1987) *Nature (London)* **328**, 834–836.
41. Rossmann, M. & Argos, P. (1975) *J. Biol. Chem.* **250**, 7525–7532.
42. Demaret, J.-P., Chwetzoff, S. & Brunie, S. (1990) *Protein Eng.* **4** (2), 171–176.
43. Kuipers, O. P., Thunnissen, M. M. G. M., de Gues, P., Dijkstra, B. W., Drenth, J., Verheij, H. M. & de Haas, G. H. (1989) *Science* **244**, 82–85.